Food Hydrocolloids 48 (2015) 292–300

Contents lists available at ScienceDirect

Food Hydrocolloids

journal homepage: www.elsevier.com/locate/foodhyd

Development and characterization of lactoferrin-GMP nanohydrogels: Evaluation of pH, ionic strength and temperature effect

Ana I. Bourbon [a], Ana C. Pinheiro [a], Maria G. Carneiro-da-Cunha [b], Ricardo N. Pereira [a], Miguel A. Cerqueira [a, *], António A. Vicente [a]

[a] CEB – Centre of Biological Engineering, Universidade do Minho, Campus de Gualtar, 4710-057 Braga, Portugal
[b] Departamento de Bioquímica, Laboratório de Imunopatologia Keizo Asami (LIKA), Universidade Federal de Pernambuco, Av. Prof. Moraes Rego, s/n, Cidade Universitária, CEP 50.670-420 Recife, Pernambuco, Brazil

ARTICLE INFO

Article history:
Received 16 September 2014
Received in revised form
4 February 2015
Accepted 9 February 2015
Available online 5 March 2015

Keywords:
Milk proteins
Biopolymer nanoparticles
Electrostatic interaction
Thermal gelation
Whey proteins

ABSTRACT

Lactoferrin (Lf) and glycomacropeptide (GMP), two bioactive proteins from milk, were used to produce nanohydrogels by electrostatic interaction and thermal gelation. Parameters such as protein concentration, molar ratio, pH, temperature and heating time were evaluated in order to develop the nanohydrogels, which were characterized in terms of morphology (Transmission Electron Microscopy – TEM, Dynamic Light Scattering – DLS, Atomic Force Microscopy – AFM and Confocal Laser Scanning Microscopy – CLSM) and stability. The aggregation of the mixture between Lf and GMP increased with the increase of temperature, resulting in particles with lower hydrodynamic diameter and polydispersity index (PdI). Nanohydrogels were obtained from the mixture of Lf and GMP solutions (0.02% (w/w) in molar ratio 1:7) at pH 5.0, and subsequently stirred and heated at 80 °C, during 20 min. Results showed that nanohydrogels have a spherical shape with a hydrodynamic diameter around 170 nm, a PdI of 0.1 and a swelling ratio of 30. The minimum size of nanohydrogels depends on protein concentration and molar ratio. Decreasing the protein concentrations and increasing the content of GMP molecules in solution, the hydrodynamic diameter and PdI of nanohydrogels decreased. The electrical charge values of nanohydrogels at different pH values suggest that Lf molecules are in the surface and GMP molecules are mostly in the core of the structure (confirmed by confocal microscopy). Also, it was observed that nanohydrogels' hydrodynamic diameter and PdI, after formation, are influenced when submitted at different conditions of pH, ionic strength and temperature. Lf-GMP nanohydrogels showed properties that indicate that they are a promising delivery system for food and pharmaceutical applications.

1. Introduction

One of the challenges in food engineering is the development of safe bio-systems that can protect, carry and deliver functional food components, which can be achieved using natural polymers. Protein-based nanohydrogels have attracted considerable attention due to their non-toxicity, biodegradability and small dimension with a large interior network for multivalent bioconjugation, which offers several possibilities for the encapsulation of functional components by covalent bonds (Bengoechea, Peinado, & McClements, 2011; Daniel-da-Silva, Ferreira, Gil, & Trindade, 2011). Food protein nanohydrogels are a network stabilized by hydrophobic interactions, disulfide bonds, and hydrogen bonds resulting from gelation process. During the heat induced gelation, the native protein conformation becomes unfolded (exposing functional groups such as sulfhydryl or hydrophobic groups) and the aggregation process occurs through disulfide bonds and hydrophobic interactions, in order to minimize the energy of the system. Then a large increase in elasticity occurs, resulting from the formation of multiple hydrogen bonds upon cooling (Batista, Portugal, Sousa, Crespo, & Raymundo, 2005). However gelling can also occur in the absence of sulphydryl/disulphide interchange reactions. In this case hydrogen bonding, electrostatic and hydrophobic interactions can be important in protein aggregation.

Lactoferrin (Lf) is a basic, positively charged iron-binding glycoprotein of the transferrin family with a molecular weight of 80 kDa and an isoelectric point around 7.8–8.5, present in various external secretions of mammals such as milk (Brisson, Britten, &

* Corresponding author. Tel.: +351 253 601962/601986; fax: +351 253 604429.
E-mail address: miguelcerqueira@deb.uminho.pt (M.A. Cerqueira).

http://dx.doi.org/10.1016/j.foodhyd.2015.02.026
0268-005X/

Pouliot, 2007; Tokle, Decker, & McClements, 2012; van der Strate, Beljaars, Molema, Harmsen, & Meijer, 2001). One of the main interests in Lf resides in its various biological activities such as: antimicrobial, anti-inflammatory, antitumour, immunomodulatory and enzymatic activities, increasing the interest in its use as a natural bioactive ingredient in food and health products (Brisson et al., 2007; González-Chávez, Arévalo-Gallegos, & Rascón-Cruz, 2009). Casein-macropeptide (CMP) is one of the most abundant peptides in cheese whey with typical concentrations between 15% and 25% of total whey proteins (El-Salam, El-Shibiny, & Buchheim, 1996). Glycosylated CMP (GMP) represents about 50% of the total CMP and exhibits high carbohydrate content (N-acetylneuraminic acid (sialic acid), galactose, and Nacetylgalactosamine) without aromatic amino acids. It is an acidic peptide with isoelectric point between 4 and 5, highly soluble in water and heat stable (Thomä-Worringer, Sørensen, & López-Fandiño, 2006). GMP has been reported to have a wide range of bioactive properties such as: antibacterial activity, modulation of immune system responses and control of blood circulation (Thomä-Worringer et al., 2006). Due to its biological activities and high potential as an ingredient for functional food and pharmaceuticals, great attention has been given to GMP application in recent years (Nakano & Ozimek, 2000; Thomä-Worringer et al., 2006; Xu, Sleigh, Hourigan, & Johnson, 2000).

Interactions between natural biopolymers, such as peptides or proteins, under specific conditions (e.g. pH, temperature, heating time, ionic strength and concentration) can promote the formation of hydrogels with improved functional properties in comparison with those of proteins alone. These biopolymer-based nanohydrogels must be carefully designed and manufactured so that they exhibit the required functional attributes within the final product (e.g. optical properties, rheological properties, release characteristics, encapsulation properties and physicochemical stability) (Jones & McClements, 2010). In this process, the biopolymer selection to form nanohydrogels will depend on a number of factors, such as: biopolymers characteristics (e.g. molecular weight, types of structure (globular or linear proteins), solubility, charge and isoelectric point) and preparation technique (e.g. heat induced gelation, use of cross-linkers, effect of pH and ionic strength). These factors are extremely important to control the ability of biopolymers to assemble into particles, influencing their functional attributes (e.g. size, structure, charge, permeability, and stability to environmental and solution conditions) (Morimoto, Nomura Shinichiro, Miyazawa, & Akiyoshi, 2006; Schmitt et al., 2009; Yu, Yao, Jiang, & Zhang, 2006). This research work provides important information on the effect of specific conditions (such as temperature, concentration and ionic strength) in the development of nanohydrogels from a globular protein (Lf) and a glycosylated peptide (GMP) which can be useful for the design of e.g. nano-structures for food and pharmaceutical applications.

2. Materials and methods

2.1. Nanohydrogel preparation

Purified Lf powder was obtained from DMV International (USA). The reported composition expressed as a dry weigh percentage was: 96% protein, 0.5% ash, 3.5% moisture and an iron content around 120 ppm. Commercial GMP was obtained from Davisco Food International, INC. (Le Sueur, USA) and its reported composition was: 82.5% protein, 1% fat, 7% ash and 7% moisture.

Lf and GMP aqueous solutions were prepared separately (with concentrations in the range of 0.02–2.0% (w/w)) using deionized water purified to a resistance of 15 MΩ (Millipore, France). Protein solutions were prepared by adding deionized water to a weighted amount of Lf or GMP powder and then stirring (60 rpm) at room temperature (25 °C) for 1 h. The pH values of biopolymer solutions were separately adjusted to 5.0, with 0.1 mol/L hydrochloric acid (Panreac, Spain). Lf aqueous solution was added dropwise into GMP aqueous solution with gently stirring until final molar ratio (MR) of Lf to GMP ranging between 1:7, 1:4 and 1:2.

After gentle stirring for 30 min, the pH of the mixture was adjusted to different values of pH (ranging between 2.5 and 10.5) with 0.1 mol/L hydrochloric acid or sodium hydroxide (Riedel-de Haen, Germany). The mixture was subsequently heated at 60, 70 or 80 °C for 10, 30 or 60 min in a water bath (closed system) to obtain a homogeneously dispersed nanohydrogel solution. The solutions were stored at 4 °C until further utilization. All the experiments in which were tested the stability of environmental conditions on nanohydrogels properties, were performed with an incubation time of 48 h, in order to ensure the stability of particles (i.e. after this time the nanohydrogels did not show any change in hydrodynamic diameter and charge).

2.2. ζ-potential

ζ-potential measurement was carried out at room temperature (25 °C) on a Zetasizer Nano ZS (Malvern Instruments, UK) in a folded capillary cell using a He–Ne laser-wavelength of 633 nm and a detector angle of 173°. The measurements were made in triplicate, with three readings for each sample. The results are given as the average ± standard deviation of nine measurements.

2.3. Nanohydrogel hydrodynamic diameter and polydispersity index

The mean hydrodynamic diameter of nanohydrogels was determined by dynamic light scattering (DLS) in a Zetasizer Nano ZS (Malvern Instruments Limited, UK). Cycles of temperature were also performed using DLS; at each temperature the sample was equilibrated at least 2 min before measurement. Each sample was analysed in cuvettes with a path length of 12 mm. The values reported correspond to polydispersity index (PdI) and Z-average diameter, that is, the mean hydrodynamic diameter, and represent the average ± standard deviation of nine measurements.

The swelling ratio of the nanohydrogels was calculated based on the ratio of the wet volume to the dry volume. Wet volume was estimated based on the hydrodynamic diameter obtained by DLS measurements and dry volume was estimated based on diameter obtained by TEM and AFM measurements. The diameter of dried nanohydrogels was determined by measuring diameters of 100–150 particles in a TEM and AFM images, using ImageJ 1.48v program.

2.4. Quartz Crystal Microbalance (QCM)

QCM measurements were carried out in a multi-frequency quartz crystal microbalance (QCM 200, Stanford Research Systems, SRS, USA), equipped with AT-cut quartz crystals (5 MHz) with optically flat polished titanium/gold electrodes in contact and liquid sides. Adsorption measurements were carried out by alternate immersion of the crystal into 0.2 mg/mL Lf (pH 5.0) and GMP (pH 5.0) solutions, for 15 min. The variations of resonance frequency (ΔF) and of the motional resistance (ΔR) were simultaneously measured as a function of time; analyses were made in triplicate at 25 °C (Pinheiro et al., 2012).

2.5. Visible (vis) absorbance

Changes of transparency of Lf-GMP mixtures with a WR of 1:2 were recorded at 600 nm in a spectrophotometer with controlled

temperature (Lamda 35, Perkin–Elmer, Germany) at 25, 60, 70 and 80 °C with deionized water as blank.

2.6. Fluorescence measurements

Fluorescence measurements were performed at 25 °C using a spectrofluorimeter (Horiba Scientific, USA) equipped with a standard thermostated cell holder. The excitation wavelength was 290 nm. Emission spectra were recorded between 300 and 400 nm with 1% attenuation, and fluorescence intensities were recorded every 0.5 nm. Excitation and emission slits were 15 nm. Data analysis of fluorescence peak was performed with Peak Fit 4.12 (SYSTAT Software Inc., Richmond, CA, USA) program.

2.7. Atomic Force Microscopy (AFM)

AFM samples were prepared by drying the solution naturally on a freshly cleaved mica surface at room temperature (25 °C). Images were acquired in tapping mode on a Digital Instruments NanoscopeIIIa (Veeco Instruments, USA).

2.8. Transmission Electron Microscopy (TEM)

TEM micrographs were conducted on a Zeiss EM 902A (Thornwood, N.Y., USA) microscope at an accelerating voltage of 50 kV and 80 kV. The samples were prepared by dropping nanohydrogel solutions onto copper grids coated with carbon film and followed by natural drying.

2.9. Confocal laser scanning microscopy

Confocal laser scanning microscopy (Olympus Fluoview, FV 1000, USA) was used to visualize the distribution of Lf and GMP in nanohydrogels. Lf and GMP were labelled with Fluorescein Isothiocyanate – FITC (Fluka, Germany) and Rhodamine B Isothiocyanate – RBITC (Sigma–Aldrich, USA), respectively. Briefly, the pH of each protein solution (2 mg/mL) was adjusted to 9.3 via dialysis against 2 L of 100 mM sodium carbonate pH 9.3, at 24 °C for 24 h 0.0015 g of a FITC or Rhodamine solution (3 mg of corant in 1 mL of 100 mM sodium carbonate pH 9.3) was added to the protein solution and incubated at 20 °C for 1 h. Unattached corant was removed by dialysis (cut off 100–500 Da; Spectra/Por CE; Spectrum laboratories; USA). After staining proteins, nanohydrogels were prepared as described before (please see Section 2.1). In order to identify each protein, the laser was adjusted to green (FITC-labelled lactoferrin) or red (RBITC-labelled GMP) mode which yielded two excitation wavelengths at 488 (green laser) and 561 nm (red laser), respectively. The superposition of the images obtained in these two channels allowed visualizing the protein distribution in nanohydrogels, in the same image.

2.10. Native polyacrylamide gel electrophoresis (Native-PAGE)

In order to evaluate the heat treatment effects on nanohydrogel kinetic formation, patterns of Lf, GMP and Lf-GMP mixtures samples were analysed using Native-PAGE or “nondenaturing” gel electrophoresis. Native-PAGE analyses were carried out using the Mini-Protean II dual slab cell system equipped with a PAC 300 power supply (Bio-Rad Laboratories, Hercules, CA, USA). The resolving and stacking gel contained 10 and 4% of polyacrylamide, respectively. The gels were stained with silver nitrate methodology (Chevallet, Luche, & Rabilloud, 2006). Standard marker proteins PageRuler Unstained Broad Range Protein Ladder from Thermo Scientific, was used to identify molecular weight of samples.

2.11. Influence of environmental stresses on nanohydrogels stability

pH stability: The influence of pH on nanohydrogels stability was determinate by preparing a series of samples with aqueous solutions adjusted to values ranging from pH 2 to 10 using either 0.1 mol/L HCl or 0.1 mol/L NaOH.

Salt stability: The influence of ionic strength on nanohydrogels stability (pH 5.0, at 25 °C) was examined by adding 0–200 mM NaCl to nanohydrogels after preparation.

Temperature stability: The influence of temperature on nanohydrogels stability (pH 5.0) was examined in DLS as explained in Section 2.3.

Stability of nanohydrogels throughout time: Nanohydrogels solutions were stored at 4 °C and their hydrodynamic diameter and PdI was evaluated by DLS during five months.

2.12. Statistical analyses

Statistical analyses of the data were carried out using Analysis of Variance (ANOVA) and Tukey mean comparison test ($p < 0.05$) (Statistica® 7, Statsoft, Tulsa, OK, USA).

3. Results and discussion

3.1. Electrostatic properties of the biopolymers

In order to evaluate the pH conditions that promote the development of electrostatic interactions between Lf and GMP, ζ-potentials of individual solutions of each biopolymer and of the product of ζ-potential values from the two solutions were determined (Fig 1A).

Lf solution showed a change in its charge from positive ζ-potential (13.5 ± 1.4 mV) at pH 1.5 to negative ζ-potential (−19.3 ± 1.5 mV) at pH 10.0, with a point of zero charge around the pH 7.7, as reported in previous publications (Bengoechea, Peinado, et al., 2011; McCarthy, Kelly, O'Mahony, & Fenelon, 2014; Tokle et al., 2012). On the other hand, GMP charges ranged between 20.81 ± 1.47 and −41.12 ± 4.98 mV for pH ranging between 1.5 and 10.0. The isoelectric point was found to be at pH 3.7, which is in agreement with other reported values (Thomä-Worringer et al., 2006). The product of ζ-potentials reaches a minimum at pH 5.0, indicating that the strongest electrostatic attraction between these two biopolymers should happen at this pH value.

Electrostatic interactions between Lf and GMP were clearly seen by QCM measurements (Fig. 1B) in which the response signal (of resonant frequency – Delta F) changes are assumed to be proportional to the mass of substance deposited to the electrode surface (Pinheiro et al., 2012). Fig. 1B shows the consecutive decrease of frequency after the alternate immersion of the crystal in Lf and GMP solutions, which means that mass is being subsequently deposited confirming the electrostatic interaction between these biopolymers.

3.2. Effect of heating temperature and time on nanohydrogel formation

In order to evaluate the influence of thermal process on nanohydrogels formation, a heat treatment at different temperatures and time were carried out to induce intermolecular hydrophobic association and promote the association between Lf and GMP. Heating individual solutions of Lf or GMP do not show a significant change ($p > 0.05$) in transparency values, indicating that no significant aggregation happened when protein solutions were treated alone (Fig. S.1). From Table S.1 and Table S.2 is possible observe the effect of temperature on hydrodynamic diameter and

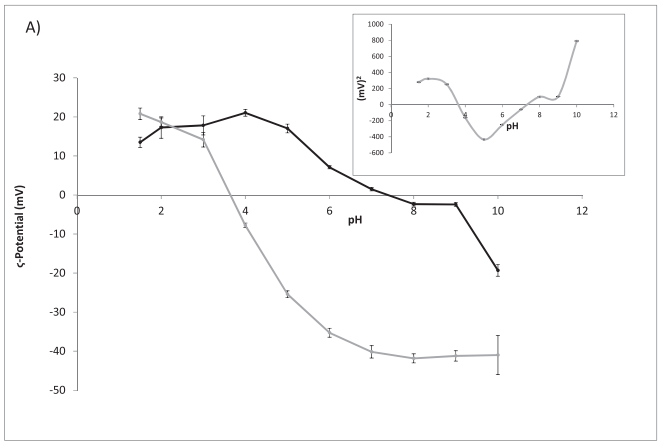

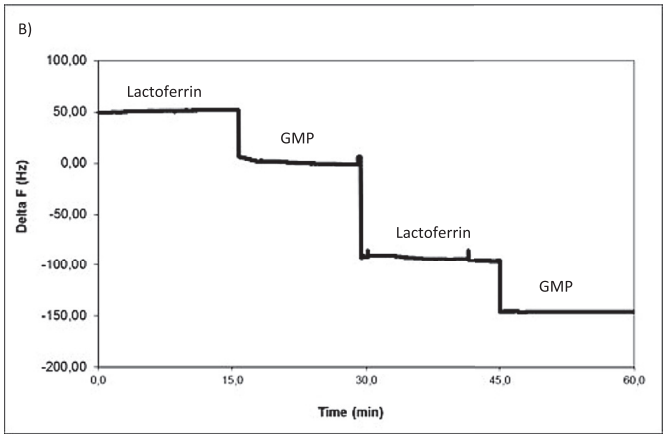

Fig. 1. Electrostatic properties of biopolymers: A) ζ-Potential of Lf (●) and GMP (●) solutions as a function of pH. Inset figure shows the product of these ζ-potentials (molar ratio of 1:4) from pH 1.5 to 10.0. Each data point is the average and the error bars show the standard deviation, B) QCM response signal (resonant frequency, Delta F) for the sequential adsorption of Lf and GMP onto a gold electrode surface at pH 5.0.

PdI values of Lf and GMP individual solutions, respectively. Increasing temperature did not show a significant change in hydrodynamic diameter of protein solutions. Furthermore, it is possible observe that Lf and GMP solutions present a high value of PdI suggesting that these solutions are not monodisperse. However, when the mixture of the two proteins is submitted to the heating treatment, a gradual decrease of transparency is observed with the increase of temperature from 60 to 80 °C (Fig. S.1). During the gelation process, it is possible observe that the decrease of transparency is proportional to the decrease of hydrodynamic diameter and PdI values obtained for Lf-GMP mixtures (Table S.3).

It also was observed that the increase of temperature led to a faster and more extensive aggregation of the mixture. The transparency decrease is presumably an indication of changes in the conformation and aggregation state of proteins during heating: when proteins unfold, they expose nonpolar groups normally buried in their non-polar interior, which leads to aggregation through hydrophobic attraction (Hoffmann, Sala, Olieman, & de Kruif, 1997). We believe that this behaviour is due the presence of globular protein (Lf) once GMP structure did not change with temperature, as expected for a peptide. Bengoechea, Jones, Guerrero, & McClements (2011), Bengoechea, Peinado, et al (2011) showed by DSC that native Lf has two thermal transitions: the first transition around 65.1 °C corresponding to the apo-lactoferrin form and the second transition around 89–92 °C which corresponds to the holo-lactoferrin form (Bengoechea, Peinado, et al., 2011). In this work, the authors pre-heated Lf at 75 °C for 20 min (a temperature which is between the two thermal denaturation peaks) in order to avoid the completely denaturation of protein and when analysed the turbidity measurements they observed that the turbidity remained relatively constant and close to zero when the samples were heated from 25 to 60 °C. However a pronounced increase in turbidity occurred from 60 to 80 °C, suggesting that the observed increases in turbidity correspond to protein aggregation induced by thermal denaturation of the globular proteins. We believe that as reported by these authors, the effect of this temperature range is due the conformational changes on Lf structure.

Also, Brisson et al. (2007) analysed that heating holo-Lf at 80 °C led to soluble polymer formation whereas apo and native Lf associated into large insoluble aggregates. The thermal aggregation of holo-Lf was mainly driven by non-covalent interactions, with intermolecular thiol/disulphide reactions also observed above 80 °C (Brisson et al., 2007).

The effect of heating time and temperature in the Lf-GMP mixture properties was also evaluated by DLS (Fig. 2). Fig. 2A shows that after 10 min of heating, nanohydrogels are formed and the increase of heating time for each temperature results in a PdI decrease, resulting in homogeneous nanohydrogels solutions (PdI < 0.2). Results also show that for a temperature of 80 °C during

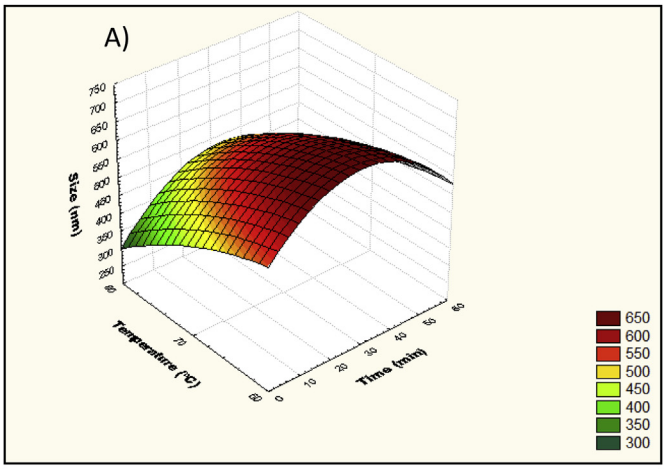

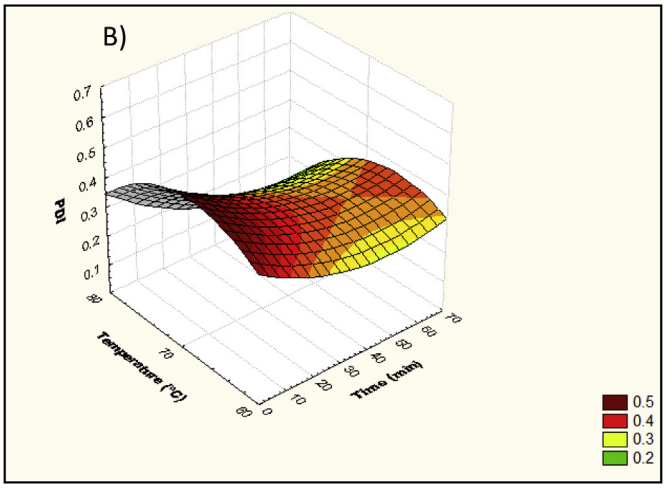

Fig. 2. Effect of temperature and heating time on the: A) hydrodynamic diameter (size) and B) polydispersity index (PdI) of Lf-GMP nanogels (0.02% (w/w), molar ratio of 1:4 and at pH 5.0).

20 min and a molar ratio of 1:7 Lf to GMP, the nanohydrogels were formed with a minimal hydrodynamic diameter and PdI values (320 ± 10 nm and 0.12 ± 0.03, respectively), with a single peak in the size distributions (results not shown). These experiments are useful for determining optimum processing conditions required to form Lf-GMP nanohydrogels by thermal processing. If the time is too short, then protein aggregation will not have fully occurred. On the other hand, if the time is too long, there will be unnecessary energy and time costs (Benichou, Aserin, Lutz, & Garti, 2007).

In order to analyse the effect of heating time on the conformational and structural changes of Lf and Lf-GMP mixtures, intrinsic fluorescence of tryptophans (Trp) residues was performed. Trp fluorescence wavelength is known to be sensitive to the polarity of its local being a useful tool to monitor changes in proteins and to make inferences regarding local structure network and dynamics (Uversky, Narizhneva, Kirschstein, Winter, & Löber, 1997; Vivian & Callis, 2001).

It was observed that the averaged emission fluorescence spectra for Trp, presented a typical maximum near to 336 nm representing the emission band Trp which is presented in different parts of the Lf, in agreement with data reported in the literature (Fang et al., 2014).

The changes in the fluorescence intensity and wavelength of the maximum intrinsic fluorescence spectrum (λ_{max}) was used to follow the structural changes of the protein induced by heating time at 80 °C. An increase of fluorescence intensity at λ_{max} was observed increasing the heating time of protein solutions at 80 °C during 20 min (Fig. 3A). This difference in fluorescence intensity as a function of heating time reflects changes in the compactness of the protein molecule due to molecules unfolding, and increasing accessibility of Trp residues. As shown in Fig. 3A it was also observed that Lf used as control has a higher fluorescence intensity than Lf-GMP mixtures, suggesting that the interaction between these two molecules are influencing the accessibility of Trp residues presented in Lf. For instance, LF used as control had a λ_{max} at about 336.2 nm while the λ_{max} of LF–GMP mixtures was significantly blue-shifted to 331.6 nm (see Fig. 3B). The blue-shift of λ_{max} suggests that Trp residues are less exposed to the solvent being placed in the nonpolar core of the system Lf-GMP (Uversky et al., 1997).

A native electrophoreses was performed in order to evaluate the kinetic formation of Lf-GMP nanohydrogels during 20 min at 80 °C (Fig. 4). Electrophoresis profile of Lf (lane 1) revealed the presence of other proteins bands, reflecting the partial purity of the Lf used. Lf was identified as the band at 79 KDa. This profile and molecular weight were also observed by other authors (Bourbon et al., 2011; Lindmark-Månsson, Timgren, Aldén, & Paulsson, 2005). The analysis of GMP (lane 2) gave a unique band with a mass of 25 KDa, corresponding to GMP. Lane 3 corresponds to the electrophoresis profile of Lf-GMP mixture without heating treatment and it is possible to observe the presence of two bands: the lower band indicate the GMP presence and the higher band reflects the LF presence. Lane 4, 5, 6 and 7 is the kinetic formation of nanohydrogels during the heating time of 5, 10, 15 and 20 min at 80 °C, respectively. It is possible to observe that after 10 min, occurs the aggregation of Lf and GMP protein. This is traduced by the appearance of a new smear band with much higher molecular weight, suggesting formation of a nanohydrogel network.

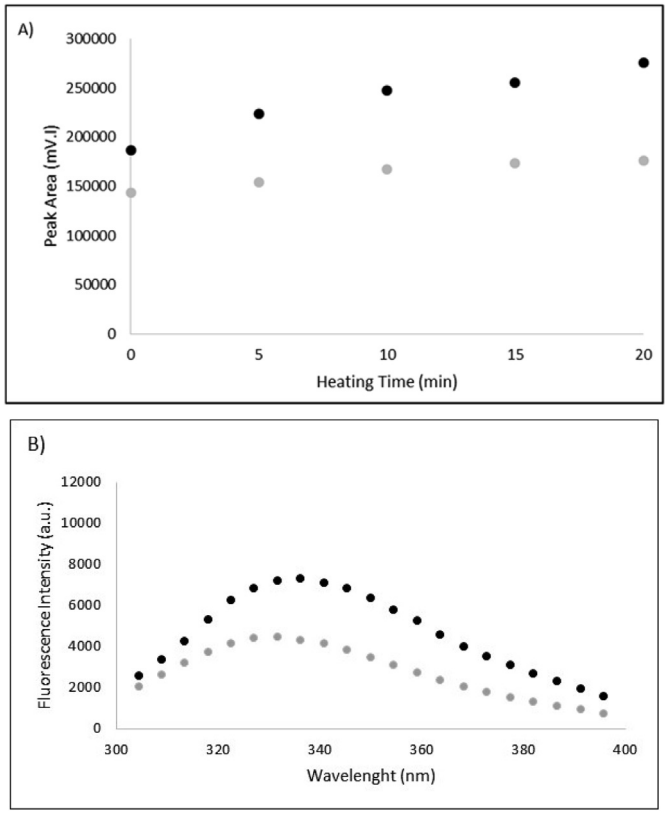

Fig. 3. Structural changes of Lf and Lf-GMP mixture monitored by: A) peak area of intrinsic fluorescence emission during heating time at 80 °C for Lf (●) and Lf-GMP mixture (●); B) Intrinsic fluorescence emission spectra of Lf solution (●) and LF-GMP mixture (●) heated at 80 °C during 5 min.

3.3. *Effect of biopolymer concentration and molar ratio (MR) on the formation of Lf-GMP nanohydrogels*

In this section, the influence of Lf and GMP concentrations and MR on the hydrodynamic diameter and PdI of the nanohydrogels was analysed. Initially, was evaluated the effect of increasing protein concentrations for a MR of 1:4 of Lf to GMP. Results showed that higher protein concentration leads to increasing hydrodynamic diameter values, from 320 ± 10 nm to 5.0 ± 0.2 μm for 0.02–2.0% (w/w) protein concentration, respectively. The effect of protein concentration on hydrodinamic diameter was already reported by other authors, which pointed out an increase in particles diameter with increased biopolymer concentration (Hu, Yu, & Yao, 2007).

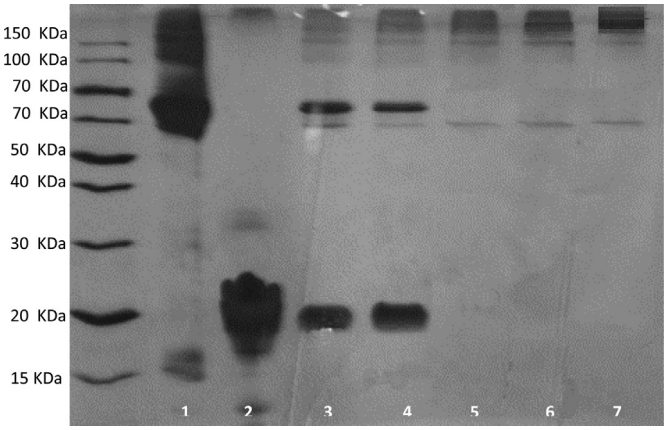

Fig. 4. Native-PAGE analysis of Lf (1), GMP (2), unheated mixture of Lf and GMP (3) and heated mixture of LF-GMP mixture during 5, 10, 15 and 20 min for lane 4, 5, 6 and 7, respectively.

The interactions between Lf and GMP depend not only upon the protein concentration of the solution but also upon their ratio of mixture. Therefore, different WR were evaluated for 0.02% of Lf and 0.02% of GMP (concentration that allow the lower values of hydrodynamic diameter and PdI of nanohydrogels). Hydrodynamic diameters decrease when the ratio of Lf to GMP (MR) is 1:7, together with a PdI around 0.1 and a single peak in the size distribution.

Anema and de Kruif (2012) evaluated the interaction between Lf and κ-casein in order to obtain stable complexes coacervates, and observed that 1 molecule of Lf interact for 4 molecules of GMP, and at these conditions the positive charges are equal to negative charges and consequently a larger particles were formed. Based on this, and due the fact that in this work we are using a glycol-peptide obtained from K-casein, we believe that the smaller hydrodynamic diameter and PdI obtained for a MR 1:7 of Lf to GMP can be justified by the fact that at this conditions the electrostatic interactions are higher and due the hydrophilic properties and glycosylated part of the peptide, the hydrophobic interactions between Lf and GMP are more evident, reflecting a smaller and stable particle (Anema & de Kruif, 2012). Therefore, the MR of 1:7 was chosen to proceed with the study of Lf and GMP nanohydrogels (Table 1).

3.4. Characterization of Lf-GMP nanohydrogels

The morphology of nanohydrogels was observed by TEM (Fig. 5). Individual Lf and GMP solutions with the same thermal treatment used to develop nanohydrogels were analysed and it was observed that no nano spherical particles were formed (Fig. 5A and B). However, when the mixture of Lf and GMP are treated with thermal treatment, nanohydrogels are observed by TEM (Fig. 5C and D), the presence of particles with a spherical shape and with a mean diameter of 80 nm. These images confirm the formation of the Lf-GMP nanogels, corroborating the previous results, however the hydrodynamic diameter is lower than observed by DLS, this can be due to drying process of particles realized to prepare samples for TEM visualization.

Additionally, AFM images were analysed to determine the average surface roughness of each system (Fig. 6). Solutions were fixed to mica slides by desiccation of dilute sample solutions based on preliminary experiments that indicated particle structure maintenance during lyophilization. The AFM images of Lf-GMP nanohydrogels showed uniform spherical particles, with the dimensions of the structures observed being less than 70 nm and with a smooth surface.

The swelling ratio of the nanohydrogels was about 30 calculated by the ratio of the wet volume to the dry volume $(170\ nm)^3/(70\ nm)^3$. This calculate was used based on DLS measurements for the diameter of particles in solution and in TEM and AFM micrographs for dry samples (Huang, Remsen, Kowalewski, & Wooley, 1999).

3.5. Effect of environmental conditions on the stability of Lf-GMP nanohydrogels

Nanohydrogels may be exposed to a great variety of conditions when they are incorporated into products, such as foods, cosmetics, personal care products and pharmaceuticals (Bengoechea, Jones, et al., 2011). It is therefore important to establish the effect of various environmental conditions on their stability and functional properties. In this section, the nanohydrogels produced at 80 °C during 20 min, with MR 1:2, at pH 5.0 were selected based in their low hydrodynamic diameter distribution and PDI values, and the influence of environmental conditions (i.e. pH, ionic strength and temperature) on their stability were evaluated (Fig. 7).

Table 1
Effect of different weight ratio of Lf:GMP solutions in nanohydrogels formation (0.02% (w/w) at pH 5.0).

molar ratio (Lf:GMP)	Hydrodinamic diameter (nm)	PdI
1:7	170 ± 3	0.08 ± 0.01
1:4	320 ± 10	0.12 ± 0.03
1:2	487 ± 9	0.32 ± 0.01

The pH and ionic strength of the solutions were adjusted after nanohydrogels formation. Fig. 7A shows ζ-potential of nanohydrogels and of lactoferrin and GMP individually, (already showed in Fig. 1 and reported here again for comparison purposes). The electrical charge values of nanohydrogels changed from positive at low pH to negative at high pH, with a neutral charge around pH 6.0 which is close to the zero ζ-potential of Lf (Fig. 7A). This result suggests that the surface of the nanohydrogels is enriched with Lf molecules and GMP molecules are mostly in the core of the structure. These results are in agreement with the results suggested by micrographs obtained by CLSM (Fig. S.2). Two fluorescence channels, green and red lasers, were used to excite Lf and GMP, respectively (Fig. S.2). Images obtained by CLSM allow identifying the localization/distribution of Lf and GMP in the nanohydrogel structure. It was observed that the intensity of FITC-labelled Lf fluorescence was higher than the fluorescence emitted by RBITC-labelled GMP, suggesting that Lf can be more distributed in the surface of nanohydrogels and GMP molecules are enriched in the core of the nanohydrogels. Similar behaviour was reported by other authors that developed nanogels by self-assembly and thermal gelification of proteins (Jones, Decker, & McClements, 2009; Li, Yu, Yao, & Jiang, 2008; Yu, Hu, Pan, Yao, & Jiang, 2006).

Fig. 7B shows an evident effect of pH on nanohydrogels' structure. After nanohydrogels preparation, the pH of the solution in which these hydrogel particles were dispersed was adjusted to different values to evaluate its influence on their size distribution. Hydrodynamic diameter and PdI of nanohydrogels increased from pH values below 6.0 and higher than 8.0 and then decreased when pH values were in the range of 6.0–7.0. When pH is between 2.0 and 3.8, Lf is practically fully protonated, while the net negative charges of GMP decrease. For pH values of 8.0–10.0 there are electrostatic repulsions between Lf and GMP because both have net negative charges. As a consequence, the electrostatic attraction decreases causing an expansion of nanohydrogels. In the pH range of 6.0–7.0, the electrostatic attraction between Lf and GMP is higher, resulting in shrinkage of the nanohydrogels.

The addition of salt to nanohydrogels lead to the particles aggregation for lower salt concentrations, as can be seen by the increase of hydrodynamic diameter and PdI values (Fig. 7C). Ionic strength may influence Lf–GMP interactions by two mechanisms: (1) NaCl may screen the electrostatic interaction, and (2) a high concentration of NaCl may alter the structural organization of water molecules, which alters the strength of hydrophobic interactions between nonpolar groups.

For low concentrations of salt (<100 mM) it was observed that the charge of nanohydrogels is near to zero, resulting in more unstable particles which can promote the formation of aggregates (Fig. S.3). In terms of structural conformation, it was observed an increase of fluorescence intensity for nanohydrogels with salt concentrations until 100 mM, expressed by higher areas obtained for the fluorescence peak. This behaviour suggest that the Trp residues in Lf moved from an apolar environment to a more polar region and interacted with water molecules (Fig. S.4). Increasing the salt concentration (>100 mM) a decrease of nanohydrogels hydrodynamic diameter and PdI values was observed, which can be attributed to a new conformational rearrangement of proteins. Fig. S.4 shows a decrease of area peak for this range of NaCl

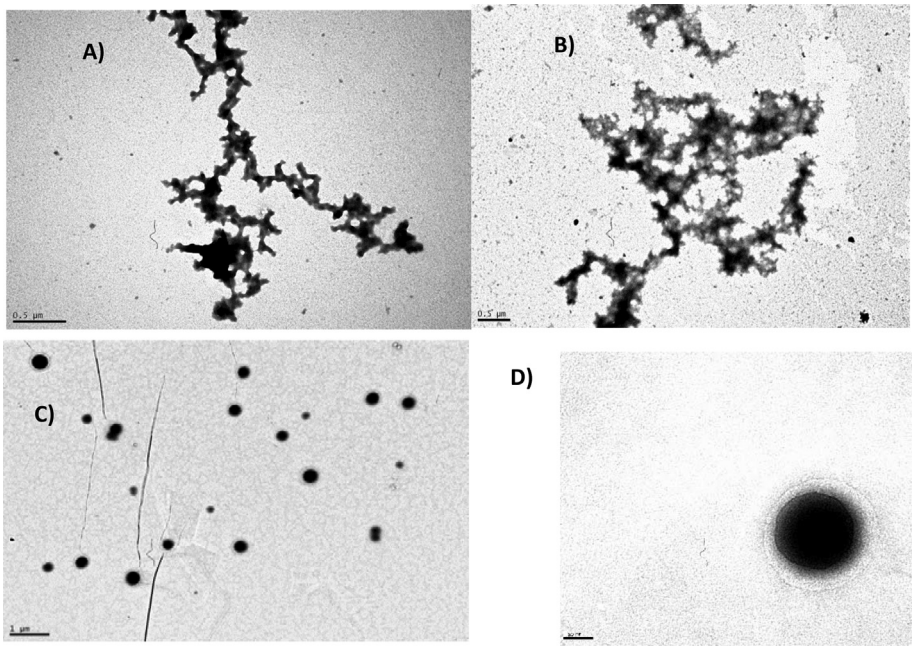

Fig. 5. TEM micrographs of Lf (A), GMP (B), Lf-GMP nanohyrogels (C) and detail (higher magnification) of Lf-GMP nanohydrogels (D). The scale bar is (A) 0.5 μm, (B) 0.5 μm, (C) 1 μm and (D) 50 nm.

concentration, reflecting the decrease of exposition of Trp residues to polar environmental. This behaviour can be due to reshuffling of protein molecular structure or to the establishment of new intermolecular associations (e.g. hydrophobic interactions) between molecules.

The effect of temperature was also assessed by heating and cooling nanohydrogel solutions at temperatures ranging from 20 to 90 °C at a rate of 10 °C/min. The particle sizes after heating and cooling cycles were analysed by dynamic light scattering (Fig. 7D). When nanohydrogels solutions were heated from 20 to 90 °C, the hydrodynamic diameter remained constant until 70 °C and increased slightly from 70 to 90 °C. This behaviour may be indicative of changes in the conformation state of nanohydrogels, corresponding to the "aggregation temperatures", as referred above. Fig. 7D shows that after cooling to ambient temperature the hydrodynamic diameter of nanohydrogels decreased.

This behaviour can be due to the re-organization of molecular structure, once in the cooling stage we are promoting an increase in elasticity, resulting from the formation of multiple hydrogen bonds and this can be reflected by the decrease of nanohydrogels size. This phenomen is usually reported in the development of proteins gels at macro scale in which during cooling stage, occurs the strengthening of the interparticle attractive non-covalent bonds such as hydrogen bonds, as the temperature decreases. This is also reported as the stabilization of the gel structure due the contribution of this kind of bonds (Ould Eleya, Ko, & Gunasekaran, 2004).

It is therefore important to establish the influence of heating on the stability and physicochemical properties of Lf-GMP nanohydrogels. The PdI values obtained ranged between 0.05 and 0.10 thus showing that size distribution is quite narrow (results not shown). A single peak was observed in the particle size distribution curves, thus leading to the conclusion that the aggregation of particles in solution was minimal.

Finally, it was evaluated the stability of Lf-GMP nanohydrogels after 5 months of storage at 4 °C (Fig. S.5B). It was observed that nanohydrogels' suspension does not change its size distribution significantly during the storage time. Also, it was possible to verify that the size distributions of the rehydrated and original nanohydrogels solutions did not show significant differences ($p > 0.05$), suggesting that the dissociation or aggregation during the process of lyophilisation and rehydration did not occur (Fig. S.5C). This result confirms that the cross-linking structure of the nanohydrogels can suppress dissociation upon dilution. In another work in which proteins (ovalbumin and lysozyme) were used to develop nanogels, it was observed that the intensities of the lyophilized and original particle solutions are somewhat different; suggesting, a limited aggregation after the lyophilisation process (Yu, Yao, et al., 2006). All these valuable characteristics can offer significant benefits for the industrial application of the nanogels.

4. Conclusions

This work has shown that at specific conditions Lf and GMP can form stable nanohydrogels. The size of the particles formed during the corresponding thermal treatment depended on protein concentration, molar ratio and temperature/time of the heating

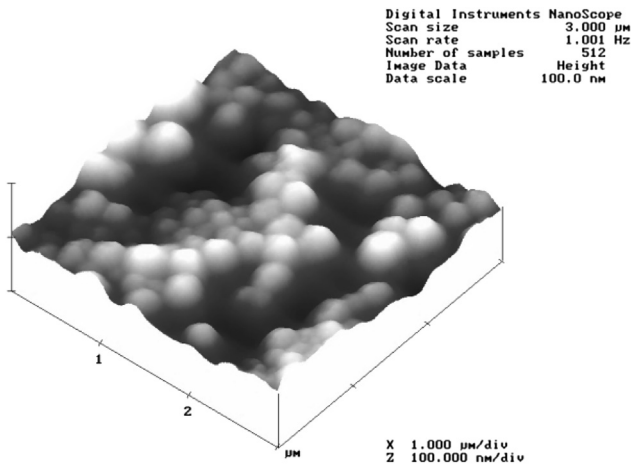

Fig. 6. AFM image of the Lf-GMP nanohydrogels.

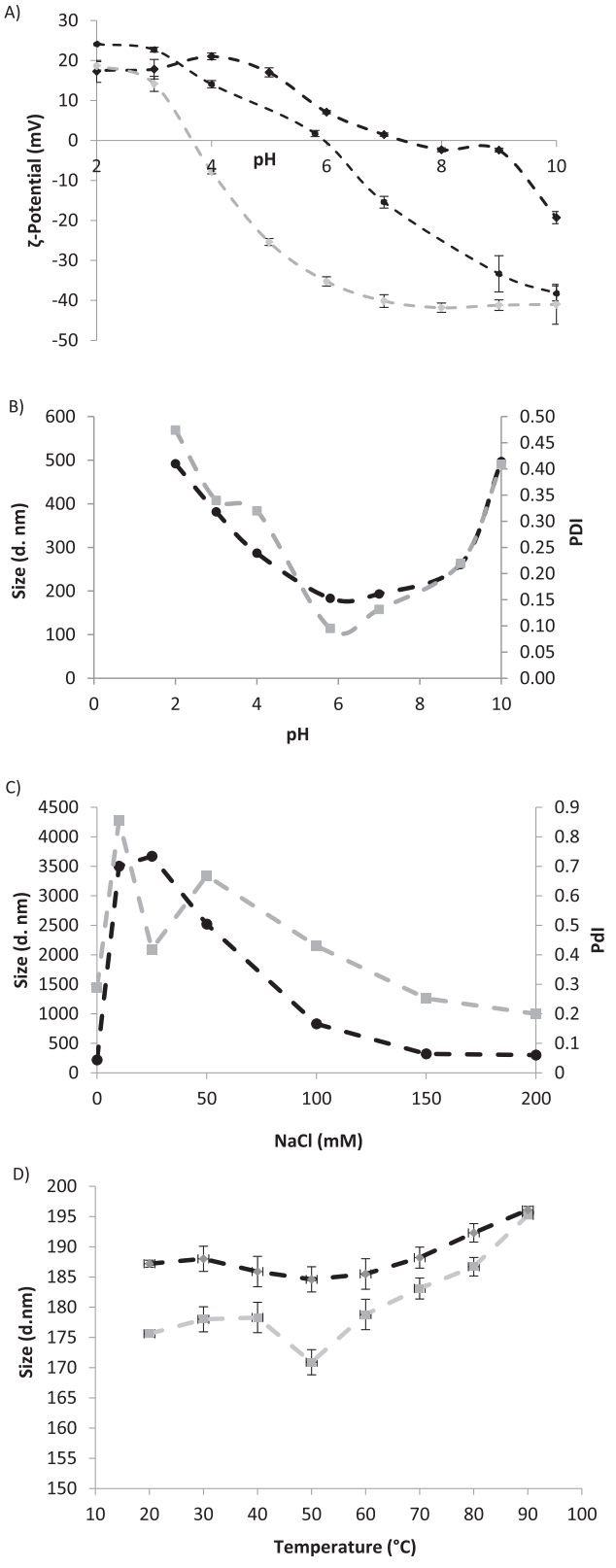

Fig. 7. Effect of environmental conditions on the stability of nanohydrogels: A) ζ-potential curves of Lf-GMP nanohydrogels (●) (curves of individual Lf (◆) and GMP (♦) are shown for comparative purposes); B) Effect of pH adjustment after heat treatment on mean particle diameter (●) and PdI (■) for Lf-GMP nanohydrogels; C) Effect of NaCl concentration on mean particle diameter (●) and PdI (■) for Lf-GMP nanogels and D) Mean particle diameter of Lf-GMP nanogels during alternate increasing (◆) and decreasing (■) temperature cycles, as measured by DLS. Dashed lines are shown for visual guidance only.

process. Results also showed that the produced nanohydrogels are stable at pH values ranging from 5.0 to 8.0 and under high temperatures and high salt concentrations. The nanohydrogels formed by thermal treatment may be useful as functional ingredients in commercial products, such as foods, cosmetics and pharmaceuticals but may also be used as a smart vehicle for bioactive compounds delivery.

Acknowledgements

The authors Ana I. Bourbon, Ana C. Pinheiro, Ricardo N. Pereira and Miguel A. Cerqueira are recipient of fellowships from the Fundação para a Ciência e Tecnologia, POPH-QREN and FSE (FCT, Portugal) through grants SFRH/BD/73178/2010, SFRH/BD/48120/2008, SFRH/BPD/81887/2011 and SFRH/BPD/72753/2010, respectively. Maria G. Carneiro-da-Cunha express is gratitude to the Conselho Nacional de Desenvolvimento Científico e Tecnológico (CNPq) for research grant. The authors would like to acknowledge to Jorge Padrão from Centre of Biological Engineering, University of Minho and André Coelho from Federal University of Ceará for helping in electrophoresis measurements and to Rui Fernandes from IBMC, University of Porto for assistance in taking the TEM pictures. Also, the authors thank the FCT Strategic Projects PEst-OE/EQB/LA0023/2013 and PEst-C/EQB/LA0006/2013 (FCT and FEDER funds through COMPETE). The work also received financial support from the European Union (FEDER funds) under the framework of QREN (Programa Operacional Regional do Norte (ON.2 — O Novo Norte; FEDER) through projects NORTE-07-0124-FEDER-000028 and NORTE-07-0124-FEDER-000069.

Appendix A. Supplementary data

Supplementary data related to this article can be found at http://dx.doi.org/10.1016/j.foodhyd.2015.02.026.

References

Anema, S. G., & de Kruif, C. G. (2012). Co-acervates of lactoferrin and caseins. *Soft Matter, 8*(16), 4471–4478.
Batista, A. P., Portugal, C. A. M., Sousa, I., Crespo, J. G., & Raymundo, A. (2005). Accessing gelling ability of vegetable proteins using rheological and fluorescence techniques. *International Journal of Biological Macromolecules, 36*(3), 135–143.
Bengoechea, C., Jones, O. G., Guerrero, A., & McClements, D. J. (2011). Formation and characterization of lactoferrin/pectin electrostatic complexes: Impact of composition, pH and thermal treatment. *Food Hydrocolloids, 25*(5), 1227–1232.
Bengoechea, C., Peinado, I., & McClements, D. J. (2011). Formation of protein nanoparticles by controlled heat treatment of lactoferrin: factors affecting particle characteristics. *Food Hydrocolloids, 25*(5), 1354–1360.
Benichou, A., Aserin, A., Lutz, R., & Garti, N. (2007). Formation and characterization of amphiphilic conjugates of whey protein isolate (WPI)/xanthan to improve surface activity. *Food Hydrocolloids, 21*(3), 379–391.
Bourbon, A. I., Pinheiro, A. C., Cerqueira, M. A., Rocha, C. M. R., Avides, M. C., Quintas, M. A. C., et al. (2011). Physico-chemical characterization of chitosan-based edible films incorporating bioactive compounds of different molecular weight. *Journal of Food Engineering, 106*(2), 111–118.
Brisson, G., Britten, M., & Pouliot, Y. (2007). Heat-induced aggregation of bovine lactoferrin at neutral pH: effect of iron saturation. *International Dairy Journal, 17*(6), 617–624.
Chevallet, M., Luche, S., & Rabilloud, T. (2006). Silver staining of proteins in polyacrylamide gels. *Nature Protocols, 1*(4), 1852–1858.
Daniel-da-Silva, A. L., Ferreira, L., Gil, A. M., & Trindade, T. (2011). Synthesis and swelling behavior of temperature responsive [kappa]-carrageenan nanogels. *Journal of Colloid and Interface Science, 355*(2), 512–517.
El-Salam, M. H. A., El-Shibiny, S., & Buchheim, W. (1996). Characteristics and potential uses of the casein macropeptide. *International Dairy Journal, 6*(4), 327–341.
Fang, B., Zhang, M., Tian, M., Jiang, L., Guo, H. Y., & Ren, F. Z. (2014). Bovine lactoferrin binds oleic acid to form an anti-tumor complex similar to HAMLET. *Biochimica et Biophysica Acta (BBA) — Molecular and Cell Biology of Lipids, 1841*(4), 535–543.

González-Chávez, S. A., Arévalo-Gallegos, S., & Rascón-Cruz, Q. (2009). Lactoferrin: structure, function and applications. *International Journal of Antimicrobial Agents, 33*(4), 301.e301–301.e308.

Hoffmann, M. A. M., Sala, G., Olieman, C., & de Kruif, K. G. (1997). Molecular mass distributions of heat-induced β-lactoglobulin aggregates. *Journal of Agricultural and Food Chemistry, 45*(8), 2949–2957.

Hu, J., Yu, S., & Yao, P. (2007). Stable amphoteric nanogels made of ovalbumin and ovotransferrin via self-assembly. *Langmuir, 23*(11), 6358–6364.

Huang, H., Remsen, E. E., Kowalewski, T., & Wooley, K. L. (1999). Nanocages derived from shell cross-linked micelle templates. *Journal of the American Chemical Society, 121*(15), 3805–3806.

Jones, O. G., Decker, E. A., & McClements, D. J. (2009). Formation of biopolymer particles by thermal treatment of [beta]-lactoglobulin-pectin complexes. *Food Hydrocolloids, 23*(5), 1312–1321.

Jones, O. G., & McClements, D. J. (2010). Functional biopolymer particles: design, fabrication, and applications. *Comprehensive Reviews in Food Science and Food Safety, 9*(4), 374–397.

Li, J., Yu, S., Yao, P., & Jiang, M. (2008). Lysozyme–dextran core–shell nanogels prepared via a green process. *Langmuir, 24*(7), 3486–3492.

Lindmark-Månsson, H., Timgren, A., Aldén, G., & Paulsson, M. (2005). Two-dimensional gel electrophoresis of proteins and peptides in bovine milk. *International Dairy Journal, 15*(2), 111–121.

McCarthy, N. A., Kelly, A. L., O'Mahony, J. A., & Fenelon, M. A. (2014). Sensitivity of emulsions stabilised by bovine β-casein and lactoferrin to heat and CaCl2. *Food Hydrocolloids, 35*(0), 420–428.

Morimoto, N., Nomura Shin-ichiro, M., Miyazawa, N., & Akiyoshi, K. (2006). Nanogel engineered designs for polymeric drug delivery. In *Polymeric drug delivery II* (vol. 924, pp. 88–101). American Chemical Society.

Nakano, T., & Ozimek, L. (2000). Purification of glycomacropeptide from dialyzed and non-dialyzed sweet whey by anion-exchange chromatography at different pH values. *Biotechnology Letters, 22*(13), 1081–1086.

Ould Eleya, M. M., Ko, S., & Gunasekaran, S. (2004). Scaling and fractal analysis of viscoelastic properties of heat-induced protein gels. *Food Hydrocolloids, 18*(2), 315–323.

Pinheiro, A. C., Bourbon, A. I., Medeiros, B. G. d. S., da Silva, L. H. M., da Silva, M. C. H., Carneiro-da-Cunha, M. G., et al. (2012). Interactions between κ-carrageenan and chitosan in nanolayered coatings—Structural and transport properties. *Carbohydrate Polymers, 87*(2), 1081–1090.

Schmitt, C., Bovay, C., Vuilliomenet, A.-M., Rouvet, M., Bovetto, L., Barbar, R., et al. (2009). Multiscale characterization of individualized β-lactoglobulin microgels formed upon heat treatment under narrow pH range conditions. *Langmuir, 25*(14), 7899–7909.

van der Strate, B. W. A., Beljaars, L., Molema, G., Harmsen, M. C., & Meijer, D. K. F. (2001). Antiviral activities of lactoferrin. *Antiviral Research, 52*(3), 225–239.

Thomä-Worringer, C., Sørensen, J., & López-Fandiño, R. (2006). Health effects and technological features of caseinomacropeptide. *International Dairy Journal, 16*(11), 1324–1333.

Tokle, T., Decker, E. A., & McClements, D. J. (2012). Utilization of interfacial engineering to produce novel emulsion properties: pre-mixed lactoferrin/β-lactoglobulin protein emulsifiers. *Food Research International, 49*(1), 46–52.

Uversky, V. N., Narizhneva, N. V., Kirschstein, S. O., Winter, S., & Löber, G. (1997). Conformational transitions provoked by organic solvents in β-lactoglobulin: can a molten globule like intermediate be induced by the decrease in dielectric constant? *Folding and Design, 2*(3), 163–172.

Vivian, J. T., & Callis, P. R. (2001). Mechanisms of tryptophan fluorescence shifts in proteins. *Biophysical Journal, 80*(5), 2093–2109.

Xu, Y., Sleigh, R., Hourigan, J., & Johnson, R. (2000). Separation of bovine immunoglobulin G and glycomacropeptide from dairy whey. *Process Biochemistry, 36*(5), 393–399.

Yu, S., Hu, J., Pan, X., Yao, P., & Jiang, M. (2006). Stable and pH-sensitive nanogels prepared by self-assembly of chitosan and ovalbumin. *Langmuir, 22*(6), 2754–2759.

Yu, S., Yao, P., Jiang, M., & Zhang, G. (2006). Nanogels prepared by self-assembly of oppositely charged globular proteins. *Biopolymers, 83*(2), 148–158.